Porous Polycaprolactone−Polystyrene Semi-interpenetrating Polymer Networks Synthesized within High Internal Phase Emulsions

Yulia Lumelsky,[†] Janet Zoldan,[‡] Shulamit Levenberg,[‡] and Michael S. Silverstein*,[†]

Department of Materials Engineering, Technion−Israel Institute of Technology, Haifa 32000, Israel, and Department of Biomedical Engineering, Technion−Israel Institute of Technology, Haifa 32000, Israel

Received December 6, 2007

ABSTRACT: PolyHIPE are highly porous, open-pore, cross-linked polymers synthesized within high internal phase emulsions (HIPE). Biodegradable polycaprolactone (PCL) oligomers were incorporated into polyHIPE using two approaches. The first approach involved copolymerization with a vinyl-terminated PCL (PCL-VL). This approach yielded a typical polyHIPE structure with voids on the order of tens of microns. The covalent bonds formed by PCL-VL prevented its removal during emulsifier extraction. The second approach involved the formation of semi-interpenetrating polymer networks (semi-IPN) with a PCL diol (PCL-OL). The relatively hydrophilic PCL-OL destabilized the HIPE and produced voids on the order of hundreds of microns, a size more appropriate for tissue engineering applications. The PCL-OL, which is more mobile than the covalently bound PCL-VL, underwent more extensive phase separation. In addition, a significant amount of PCL-OL was removed during emulsifier extraction. Cells were successfully attached to the surface of a semi-IPN polyHIPE, forming a monolayer. Eventually, spontaneous differentiation of the cells and the formation of myotubes were observed.

Introduction

Porous polymers containing biodegradable components are of interest for tissue engineering scaffolds.[1] The key parameters in scaffold selection include adequate mechanical properties, a highly porous and interconnected pore structure, a high surface area to volume ratio, and biodegradability as well as a surface chemistry that favors cellular attachment, proliferation, and differentiation.[2,3] One of the most widespread problems with the conventional methods for producing scaffolds is that the pores are not fully interconnected.[2,3] PolyHIPE are highly porous cross-linked polymers typically synthesized within water-in-oil (W/O) high internal phase emulsions (HIPE). In such HIPE, the dispersed, internal, aqueous phase (water, water-soluble initiator, and stabilizer) often occupies as much as 90% of the volume, while the continuous, external, organic phase (monomers, cross-linking comonomers, and emulsifier) often occupies as little as 10% of the volume.[4−6] The phase separation and the changes in density and in interfacial tension that can occur during polymerization cause holes to develop within the organic envelope surrounding the aqueous droplets, yielding a bicontinuous structure.[4,5] The aqueous phase can then be removed, yielding a highly porous polymer.

A variety of polyHIPE and polyHIPE-based materials have been synthesized including copolymers, interpenetrating polymer networks (IPN), crystallizable side-chain polymers, hydrogels, organic−inorganic hybrids, and composites.[4−21] PolyHIPE could have advantageous properties as tissue engineering scaffolds since they can combine a fully interconnected highly porosity structure, a low bulk density, a high permeability, and a large surface area with moduli similar to those of soft tissue.[22−27] A typical polyHIPE structure consists of spherical voids on the order of 5−30 μm (from the evacuated aqueous droplets) that are connected by holes on the order of 0.1−1 μm. Unfortunately, most tissue engineering applications require 100−500 μm pores.

The synthesis of interpenetrating polymer networks (IPN) can be used to synergistically combine the properties of two very different polymers.[28−32] Both sequential (polymerizing and cross-linking the monomer for polymer B in the presence of cross-linked polymer A) and simultaneous (polymerizing and cross-linking the monomers for polymers A and B in separate, but simultaneous, reactions) IPN have been synthesized. The individual polymer networks are interwoven on a molecular scale but not chemically linked. The thermodynamically favored phase separation in IPN is limited by the irreversibly interlocked molecular structure. The synthesis of semi-IPN is similar to the synthesis of IPN except that one of the two polymers does not undergo cross-linking. In semi-IPN, the two polymers are initially intertwined on the molecular level. However, the non-cross-linked polymer may undergo more extensive phase separation under the appropriate conditions. In fact, the non-cross-linked polymer may even be removed by swelling in an appropriate solvent.

This paper describes the synthesis of polyHIPE containing oligomers of polycaprolactone (PCL), a biodegradable polymer. In one synthesis route, the polyHIPE is cross-linked through graft copolymerization with a vinyl-terminated PCL oligomer (PCL-VL), as illustrated schematically in Figure 1a. In a second synthesis route, a semi-IPN polyHIPE containing a PCL oligomer diol (PCL-OL) is formed, as illustrated schematically in Figure 1b. The chemical structures, porous morphologies, thermal properties, and mechanical properties of the PCL-cross-linked graft copolymer polyHIPE and the PCL semi-IPN polyHIPE are compared. The results of cell growth on the semi-IPN are described.

Experimental Section

Materials. Styrene (S, Fluka Chemie) and divinylbenzene (DVB, which contains 40% ethylstyrene, Riedel-de-Haen) were washed to remove the inhibitor (three times with an aqueous solution of 5 wt % sodium hydroxide (NaOH) and then three times with deionized water). PCL-OL (M_n = 530, Aldrich) was used as

* To whom correspondence should be addressed: e-mail michaels@tx.technion.ac.il, Tel 972-4-829-4582, Fax 972-4-829-5677.
[†] Department of Materials Engineering.
[‡] Department of Biomedical Engineering.

10.1021/ma7027177 CCC: $40.75
Published on Web 01/25/2008

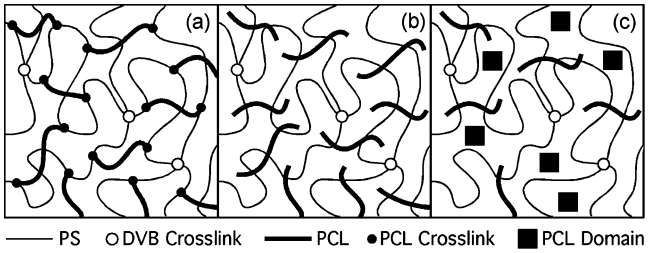

Figure 1. Schematic illustration of (a) cross-linking graft copolymer polyHIPE, (b) semi-IPN polyHIPE, and (c) phase-separated domains in semi-IPN polyHIPE.

Table 1. HIPE Compositions

		amount, wt %			
	component	S/DVB	OL-25	OL-40	VL-25
organic phase	S	8.76	6.57	5.16	6.57
	DVB	0.97	0.73	0.57	0.73
	PCL	0.00	2.43	3.82	2.43
	SMO	1.95	1.95	3.82	1.95
	total	11.68	11.68	13.37	11.68
aqueous phase	H_2O	87.64	87.64	85.96	87.64
	K_2SO_4	0.49	0.49	0.48	0.49
	$K_2S_2O_8$	0.19	0.19	0.19	0.19
	total	88.32	88.32	86.63	88.32

Table 2. Monomer Ratios

	PCL	S/DVB/PCL, wt %	S/DVB/PCL, mol %
S/DVB	none	90.0/10.0/0.0	91.8/8.2/0.0
VL-25	PCL-VL	67.5/7.5/25.0	87.0/7.7/5.3
OL-25	PCL-OL	67.5/7.5/25.0	86.1/7.6/6.3
OL-40	PCL-OL	54.0/6.0/40.0	81.0/7.2/11.8

received. For polyHIPE synthesis, the emulsifier was sorbitan monooleate (SMO, Span 80, Fluka Chemie), the water-soluble initiator was potassium persulfate ($K_2S_2O_8$, Riedel-de-Haen), and the water-soluble stabilizer used to enhance the rigidity of the interface was potassium sulfate (K_2SO_4, Frutarom, Israel).[33]

PCL-VL Synthesis. For PCL-VL synthesis, the dichloromethane (DCM, Aldrich), triethylamine (TEA, Aldrich), anhydrous magnesium sulfate ($MgSO_4$, Aldrich), potassium hydrate (KOH, Riedel-de-Haen), and hydrochloric acid (HCl, Riedel-de-Haen) were used as received, while the acryloyl chloride (AC, Aldrich) was distilled before use. The synthesis of PCL-VL from PCL-OL has been described in detail elsewhere.[34]

PolyHIPE Synthesis. The polyHIPE synthesis procedure has been described in detail elsewhere.[7] The HIPE compositions are listed in Table 1. The S/DVB/PCL mass ratios and molar ratios for the various polyHIPE synthesized are listed in Table 2. The S/DVB mass ratio was maintained at 9/1 for all the syntheses. The mass ratio of the organic phase to the aqueous phase was maintained at around 12/88 for all the syntheses. Briefly, the aqueous phase was added slowly to the organic phase (S, DVB, PCL-OL or PCL-VL, and SMO) with continuous stirring. Polymerization took place in a convection oven at 65 °C for 24 h. The polyHIPE was dried in a vacuum oven at 60 °C for about 48 h. The emulsifier, initiator, and stabilizer were removed by Soxhlet extraction in deionized water for 24 h and in methanol for 24 h. The polyHIPE was then dried in a convection oven at 60 °C for 12 h.

Characterization. The molecular structures were characterized using FTIR (from 400 to 4000 cm^{-1} at a resolution of 2 cm^{-1}, Equinox 55 FTIR, Bruker). KBr pellets containing 1 wt % were used to characterize the PCL-OL and PCL-VL. A photoacoustic attachment was used to characterize the polyHIPE. The porous structure was characterized using high-resolution scanning electron microscopy (HRSEM, Zeiss LEO 982) with uncoated specimens and an accelerating voltage of 1−3 kV. Several micrographs were analyzed for each sample to generate a statistical depiction of the average and standard deviation. The densities of the polyHIPE, ρ, were determined using gravimetric analysis. The measurements of

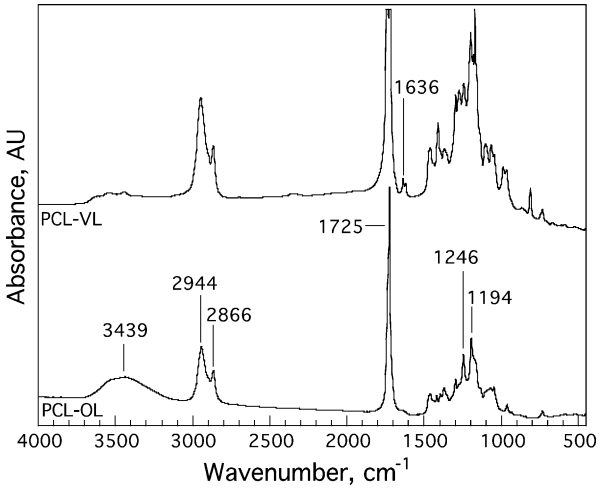

Figure 2. FTIR spectra from PCL-OL and PCL-VL.

the mass and dimensions of at least seven samples yielded an experimental error of 0.004 g/cm^3. The specific surface area was determined by the single-point BET (Brunauer, Emmett, Teller) method through nitrogen adsorption at 77 K (Quantachrome). Dynamic mechanical thermal analysis (DMTA) temperature sweeps from −100 to 200 °C were conducted at 3 °C/min and at a frequency of 1 Hz in compression (MK III DMTA, Rheometrics) on 10 mm × 10 mm × 10 mm specimens. Uniaxial compressive stress−strain measurements were conducted at 25 °C on 5 mm × 5 mm × 5 mm specimens until an equipment-related force limitation (15 N) was reached (MK III DMTA, Rheometrics).

Cell Growth. Mouse skeletal cells (c2, a gift from David Yaffe, Weizmann Institute of Science, Rehovot, Israel) were cultured according to the manufacturer's instructions. These cells, muscle satellite cells, are myoblasts (early undifferentiated skeletal muscle cells). They can remain myoblasts or, in certain conditions, can spontaneously differentiate to myotubes (more mature muscle fibers). For scaffold seeding, 1 000 000 cells were pooled and resuspended in 10 μL of a 1:1 mixture of culture medium and Matrigel (BD Biosciences) as described elsewhere.[35] Cell proliferation and growth were observed using environmental scanning electron microscopy (ESEM, FEI Quanta 200) operating in low vacuum mode. Cell-polyHIPE specimens were first fixed in a solution containing 1% glutaraldehyde and then dehydrated with hexadimethyldisilazane (HDMS, Sigma) according to the manufacturer's instructions. Uncoated samples were observed in the ESEM at 10 kV and a working distance of 10.5 mm.

Results and Discussion

PLC-VL Synthesis. Fourier transform infrared spectroscopy (FTIR) confirmed the substitution of the hydroxyl groups in PCL-OL with vinyl groups in the synthesis of PCL-VL (Figure 2). PCL-OL exhibited a broad OH stretching band at 3439 cm^{-1}.[36] PCL-VL, on the other hand, did not exhibit a broad OH stretching band at 3439 cm^{-1} but did exhibit C═C stretching bands at 1636−1620 cm^{-1} that were not present in the PCL-OL (Figure 2).[36] The strong carbonyl band at 1725 cm^{-1} and the strong ether band at 1194 cm^{-1} are typical of PCL and are not found in S or DVB.

PCL Incorporation. FTIR was also used to confirm the incorporation of PCL-VL into the graft copolymer polyHIPE and of PCL-OL into the semi-IPN polyHIPE. All the polyHIPE exhibited a band at 3022 cm^{-1} that is associated with the S/DVB benzyl CH groups (Figure 3).[36] VL-25 did not exhibit C═C bands at 1636−1620 cm^{-1}, indicating that the vinyl groups reacted during polymerization and formed a PCL-grafted polyHIPE. All the polyHIPE containing PCL exhibited a carbonyl band at 1730 cm^{-1} and an ether band at 1163 cm^{-1}.[36]

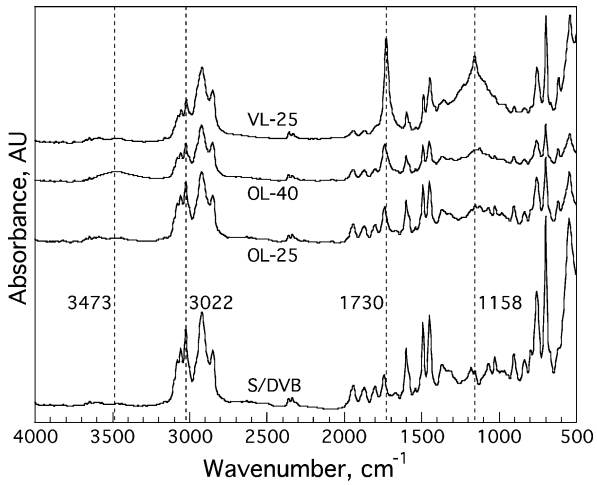

Figure 3. FTIR spectra from the various polyHIPE.

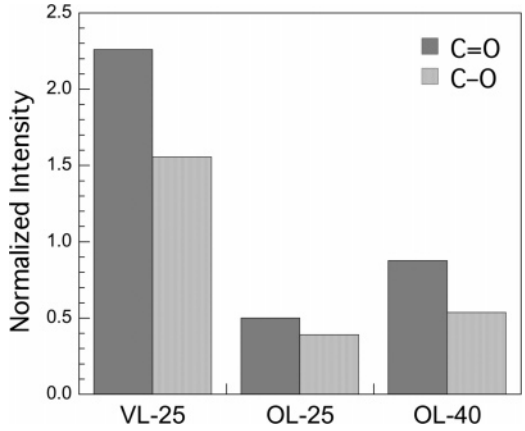

Figure 4. Intensities of the carbonyl bands at 1730 cm^{-1} and the ether bands at 1163 cm^{-1} normalized by the intensity of the CH band at 3022 cm^{-1} for the various polyHIPE.

Table 3. PolyHIPE Properties

	ρ, g/cm^3	A, m^2/g	tan δ peak, °C	E, MPa	E_w, GPa
S/DVB	0.08	2.9	162	3.8	0.56
VL-25	0.09	7.1	131	2.0	0.26
OL-25	0.06	4.4	169	1.7	0.44
OL-40	0.07	5.4	150	4.1	0.88

Neither of these bands was seen in the S/DVB control polyHIPE. In addition, the OL-40 polyHIPE exhibited a small, broad OH stretching band at 3473 cm^{-1} from the PCL-OL hydroxyl groups.

The differences in PCL incorporation between the graft copolymer and the semi-IPN become clear through a comparison of selected normalized band intensities (Figure 4). The intensities of the carbonyl band at 1730 cm^{-1} and the ether band at 1163 cm^{-1} were normalized by the intensity of the CH band at 3022 cm^{-1}. The normalized intensities of VL-25 are significantly greater than those of the corresponding semi-IPN (OL-25) and even greater than those of OL-40, with its significantly higher PCL content. These results indicate that the PCL-OL, which is not irreversibly interlocked with or covalently bound to the cross-linked polystyrene network, was removed during Soxhlet extraction of the emulsifier. In VL-25, on the other hand, the PCL is covalently bound to the polystyrene network and cannot be removed through extraction.

PolyHIPE Structure. The densities of the S/DVB polyHIPE and VL-25, 0.08 and 0.09 g/cm^3, respectively (Table 3), reflect the volume fractions of monomer in the HIPE (Table 1). The densities of the semi-IPN were lower, between 0.06 and 0.07 g/cm^3 (Table 3). The lower densities for the semi-IPN reflect the loss of PCL through extraction, as concluded from the FTIR analysis. The porous structures of the polyHIPE are seen in Figure 5. The S/DVB polyHIPE exhibits a typical polyHIPE structure (Figure 5a,b) and a typical polyHIPE surface area (2.9 m^2/g). The void diameters range from 18 to 30 μm, and the hole diameters range from 1 to 6 μm. The porous structure of VL-25 is significantly smaller but it is still a typical polyHIPE structure. The void diameters range from 4 to 7 μm, and the hole diameters range from 0.5 to 3 μm (Figure 5c,d). The density of holes within the walls (Figure 5d) is greater for VL-25 than for the S/DVB polyHIPE. This difference in the porous structure is also reflected in the larger surface area for VL-25 (7.1 m^2/g). This reduction in void and hole size may reflect a reduction in interfacial tension on the introduction of PCL, which is more polar than S and DVB.

The porous structures of the semi-IPN polyHIPE are quite different from the typical polyHIPE structure. Both semi-IPN polyHIPE contain relatively large voids, ranging between 220 and 285 μm for OL-25 (Figure 5e−g) and between 60 and 155 μm for OL-40 (Figure 5h−j). PCL-OL, with its relatively high concentration of hydroxyl groups, is significantly more hydrophilic than PCL-VL. The incorporation of significant amounts of the relatively hydrophilic macromolecular PCL-OL into the HIPE's organic phase leads to HIPE destabilization, producing the large voids in Figure 5e,h.[37] This destabilization was even more pronounced when synthesizing polyHIPE with higher PCL-OL contents, with obvious water/oil phase separation beginning as soon as the stirring ceased. In order to synthesize OL-40 with no obvious water/oil phase separation, it was necessary to double the emulsifier concentration (Table 1). The higher emulsifier content in OL-40 stabilizes the HIPE and produces a smaller void size than seen for OL-25, which has a lower emulsifier content.

The walls of the large voids in OL-25 are covered with a nodule-like structure (Figure 5g). This structure is porous, and it was possible to remove the water from the polyHIPE. Polymer−polymer phase separation yields spherical domains for a 25% PCL-OL content. This structure reflects the higher mobility of the PCL-OL which, unlike PCL-VL, can undergo extensive phase separation. The walls of the large voids in OL-40 consist of an assembly of weblike structures (Figure 5j) containing holes whose dimensions range from 0.1 to 1 μm. This structure reflects the higher PCL-OL content since polymer−polymer phase separation is expected to yield a bicontinuous structure.

Thermal and Mechanical Properties. The variations of tan δ with temperature for the various polyHIPE are seen in Figure 6 (the curves are shifted vertically for clarity). The S/DVB polyHIPE tan δ peak temperature of 162 °C (Table 3) reflects the high degree of cross-linking as well as the low thermal conductivity of the polyHIPE.[10,13] VL-25 exhibits the lowest tan δ peak temperature, 131 °C. In addition, VL-25 has a significantly lower peak height and a significantly wider peak breadth. These changes in the tan δ peak shape and position indicate that a significant amount of PCL has been incorporated into the molecular structure of the polymer network (as illustrated in Figure 1a).

The semi-IPN polyHIPE exhibit broader tan δ peaks than that of the S/DVB polyHIPE, as is commonly seen for IPN and semi-IPN systems.[28,29] The shape of the tan δ peak for OL-40 is similar to that of OL-25 but is shifted to lower temperatures, reflecting its higher PCL-OL content. OL-40 also exhibits a

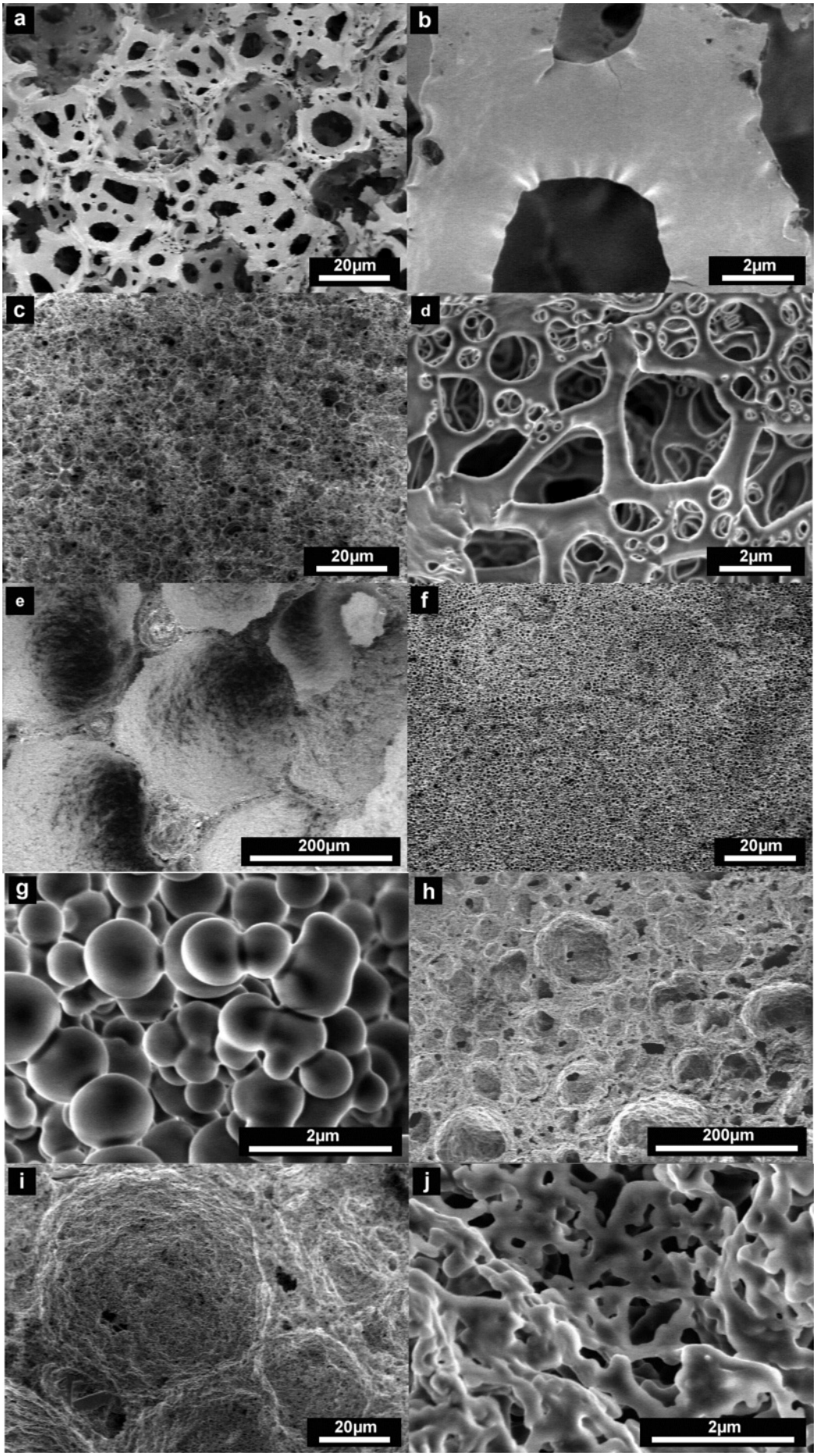

Figure 5. HRSEM micrographs of various polyHIPE fracture surfaces: (a, b) S/DVB; (c, d) VL-25; (e−g) OL-25; (h−j) OL-40.

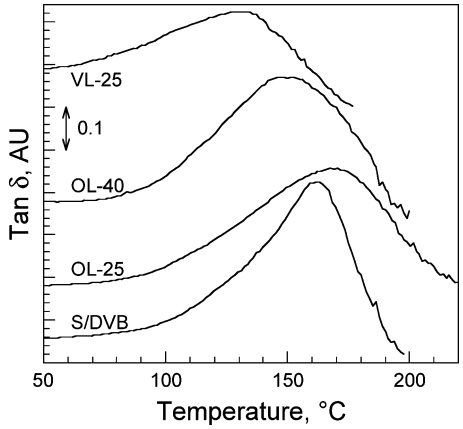

Figure 6. Variation of tan δ with temperature for the various polyHIPE.

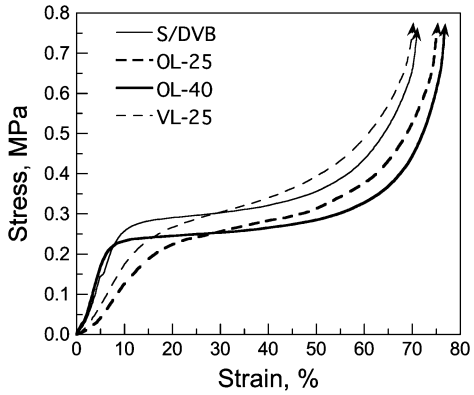

Figure 7. Compressive stress−strain curves for the various polyHIPE.

small but distinct tan δ peak at −50 °C (not shown) that is associated with the PCL glass transition temperature. The presence of a distinct PCL tan δ peak confirms that the PCL has undergone more extensive phase separation in the semi-IPN (as illustrated in Figure 1c).

In spite of the differences in the porous structures, the room temperature compressive stress−strain curves for all the polyHIPE (Figure 7) are similar, reflecting the similar densities of the polyHIPE.[38] The stress−strain curves are typical of polyHIPE, exhibiting a linear elastic region, a stress plateau region, and a densification region (with a rapid rise in stress). These curves are, in general, similar to those described by the mechanical models for open cell foams.[38] The transition points between the mechanical behavior regimes for the polyHIPE are somewhat different than those in the models. Linear elasticity is limited to small strains, typically 5% or less. The models describe the transition from the linear regime to the stress plateau regime at around 5%.[38] In the polyHIPE, however, the transition occurs between strains of 5 and 15% (Figure 7). The models indicate that the transition from the stress plateau regime to the densification regime should occur at strains around 90% for foams with densities around 0.07 g/cm^3.[38] In the polyHIPE, however, the transition occurs between strains of 70 and 80% (Figure 7).

The polyHIPE modulus, E (Table 3), was calculated from the slope at low strains. The modulus of 3.8 MPa is typical of S/DVB-based polyHIPE.[10,13] The modulus of OL-40 is similar to that of the S/DVB polyHIPE. The moduli of VL-25 and OL-25 are both lower than that of the S/DVB polyHIPE, but each for a different reason. The lower modulus for VL-25 reflects the incorporation of the relatively flexible PCL into the relatively rigid S/DVB copolymer's molecular structure. The lower modulus for OL-25 reflects its relatively low density. The moduli of the polyHIPE are of the same order of magnitude as the moduli of soft tissue (0.1−2 MPa) and are similar to the moduli of typical porous polymer systems proposed for tissue engineering applications.[39,40]

The effects of the synthesis (HIPE composition, semi-IPN vs copolymer) on the moduli of the wall materials can be derived from the moduli of the polyHIPE. The mechanical models for open cell foams relate the relative modulus (E divided by the modulus of the wall material, E_w) to the square of the relative density (ρ divided by the density of the wall material).[38] The E_w in Table 3 were calculated using the measured moduli and densities and by assuming a wall density of 1 g/cm^3 for polymers. E_w ranges from 0.26 GPa for VL-25 to 0.88 GPa for OL-40. Copolymerization with PCL-VL has been shown to enhance segmental mobility, yielding the reduction in the tan δ peak temperature. This enhancement in segmental mobility also yields the reduction in E_w. On the other hand, the formation of the OL-40 semi-IPN, which combines the relatively stiff and unmodified molecular structure of the S/DVB copolymer with a significant amount of PCL, yields an increase in E_w.

Cell Growth. The initial cell growth experiment was conducted on OL-40 (Figure 8a) since the semi-IPN contained large voids that are more conducive to cell growth and since OL-40 contained more PCL than OL-25. Cells were successfully attached to the surface of OL-40, forming a monolayer. Eventually, spontaneous differentiation of the cells and formation of myotubes (typical of skeletal cells) were seen on the surface (Figure 8b). The destabilization of the polyHIPE that

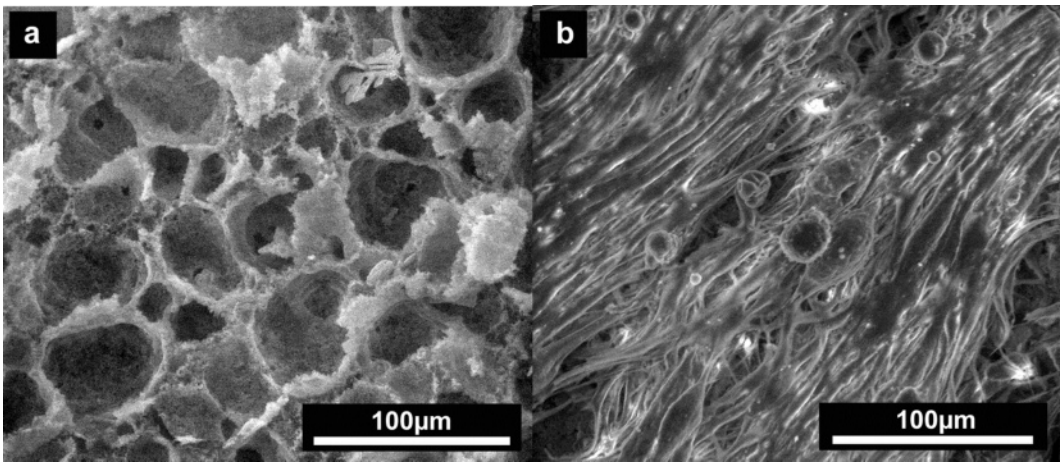

Figure 8. ESEM micrographs of OL-40: (a) as-synthesized; (b) after seeding with mouse skeletal cells.

leads to the formation of large voids has yielded porous materials that can be more suitable for tissue engineering applications than the typical polyHIPE structure. The synthesis of semi-IPN polyHIPE containing biodegradable polymers can be used to produce materials with porous structures, thermal properties, and mechanical properties that can provide alternatives to more complex syntheses.

Conclusions

Biodegradable PCL oligomers were successfully incorporated into open-pore polyHIPE, either through copolymerization with PCL-VL or through the formation of a semi-IPN with PCL-OL. Incorporation of PCL through copolymerization with PCL-VL was more effective since the formation of covalent bonds prevented the removal of PCL during the emulsifier extraction. The copolymer exhibited a typical polyHIPE structure, with void diameters ranging from 4 to 7 μm. The semi-IPN contained voids over 100 μm in diameter that resulted from the destabilization of the HIPE on addition of the relatively hydrophilic PCL-OL. The PCL-OL in the semi-IPN is not covalently linked to or physically interlocked with the cross-linked polystyrene network. The wall structure and the presence of a tan δ peak associated with PCL indicate that the PCL-OL has undergone a more extensive phase separation. The HIPE destabilization that results in the formation of relatively large voids has proven advantageous for the synthesis of porous materials that are more suitable for tissue engineering applications. Cells were successfully attached to the surface of OL-40, forming a monolayer. Eventually, spontaneous differentiation of the cells and the formation of myotubes were observed.

Acknowledgment. The partial support of the Israel Science Foundation and of the Technion VPR Fund is gratefully acknowledged.

References and Notes

(1) Ciardelli, G.; Chiono, V.; Cristallini, C.; Barbani, N.; Ahluwalia, A.; Vozzi, G.; Previti, A.; Tantussi, G.; Giusti, P. *J. Mater. Sci.: Mater. Med.* **2004**, *15*, 305.
(2) Sachlos, E.; Czernuszka, J. T. *Eur. Cells Mater.* **2003**, *5*, 29.
(3) Hutmacher, D. W. *J. Biomater. Sci., Polym. Ed.* **2001**, *12*, 107.
(4) Cameron, N. R.; Sherrington, D. C. *Adv. Polym. Sci.* **1996**, *126*, 163.
(5) Cameron, N. R. *Polymer* **2005**, *46*, 1439.
(6) Cameron, N. R.; Sherrington, D. C.; Albiston, L.; Gregory, D. P. *Colloid Polym. Sci.* **1996**, *274*, 592.
(7) Silverstein, M. S.; Tai, H.; Sergienko, A.; Lumelsky, Y.; Pavlovsky, S. *Polymer* **2005**, *46*, 6682.
(8) Sergienko, A. Y.; Tai, H.; Narkis, M.; Silverstein, M. S. *J. Appl. Polym. Sci.* **2004**, *94*, 2233.
(9) Sergienko, A. Y.; Tai, H.; Narkis, M.; Silverstein, M. S. *J. Appl. Polym. Sci.* **2002**, *84*, 2018.
(10) Tai, H.; Sergienko, A.; Silverstein, M. S. *Polym. Eng. Sci.* **2001**, *41*, 1540.
(11) Livshin, S.; Silverstein, M. S. *Macromolecules* **2007**, *40*, 6349.
(12) Kulygin, O.; Silverstein, M. S. *Soft Matter* **2007**, *2*, 1525.
(13) Tai, H.; Sergienko, A.; Silverstein, M. S. *Polymer* **2001**, *42*, 4473.
(14) Butler, R.; Davies, C. M.; Cooper, A. I. *Adv. Mater.* **2001**, *13*, 1459.
(15) Butler, R.; Hopkinson, I.; Cooper, A. I. *J. Am. Chem. Soc.* **2003**, *125*, 14473.
(16) Normatov, J.; Silverstein, M. S. *Macromolecules* **2007**, *40*, 8329.
(17) Normatov, J.; Silverstein, M. S. *Chem. Mater.*, in press (DOI:10.1021/cm0718062).
(18) Normatov, J.; Silverstein, M. S. *J. Polym. Sci., Part A: Polym. Chem.*, in press (DOI:10.1002/pola.22570).
(19) Menner, A.; Powell, R.; Bismarck, A. *Soft Matter* **2006**, *4*, 337.
(20) Haibach, K.; Menner, A.; Powell, R.; Bismarck, A. *Polymer* **2006**, *47*, 4513.
(21) Menner, A.; Haibach, K.; Powell, R.; Bismarck, A. *Polymer* **2006**, *47*, 7628.
(22) Hayman, M. W.; Smith, K. H.; Cameron, N. R.; Przyborski, S. A. *Biochem. Biophys. Methods* **2005**, *62*, 231.
(23) Hayman, M. W.; Smith, K. H.; Cameron, N. R.; Przyborski, S. A. *Biochem. Biophys. Res. Commun.* **2004**, *314*, 483.
(24) Bokhari, M. A.; Akay, G.; Zhang, S. G.; Birch, M. A. *Biomaterials* **2005**, *26*, 5198.
(25) Akay, G.; Birch, M. A.; Bokhari, M. A. *Biomaterials* **2004**, *25*, 3991.
(26) Busby, W.; Cameron, N. R.; Jahoda, C. A. B. *Polym. Int.* **2002**, *51*, 871.
(27) Busby, W.; Cameron, N. R.; Jahoda, C. A. B. *Biomacromolecules* **2001**, *2*, 154.
(28) Sperling, L. H. *Interpenetrating Polymer Networks and Related Materials*; Plenum Press: New York, 1981.
(29) Thomas, D. A.; Sperling, L. H. In *Polymer Blends*; Paul, D. R., Newman, S., Eds.; Academic Press: New York, 1978; Vol. 2.
(30) Silverstein, M. S.; Narkis, M. *J. Appl. Polym. Sci.* **1987**, *33*, 2529.
(31) Silverstein, M. S.; Narkis, M. *Polym. Eng. Sci.* **1989**, *29*, 824.
(32) Silverstein, M. S.; Narkis, M. *J. Appl. Polym. Sci.* **1990**, *40*, 1583.
(33) Pons, R.; Solans, C.; Stebe, M. J.; Erra, P.; Ravey, J. C. *Prog. Colloid Polym. Sci.* **1992**, *89*, 110.
(34) Storey, R. F.; Warren, S. C.; Allison, C. J.; Wiggins, J. S. *Polymer* **1993**, *34*, 4365.
(35) Levenberg, S.; Rouwkema, J.; Macdonald, M.; Gerfein, E.; Kohane, D.; Darland, D.; Marini, R.; van Blitterswijk, C. A.; Mulligan, R.; D'Amore, P.; Langer, R. *Nat. Biotechnol.* **2005**, *23*, 879.
(36) Colthup, N. B.; Daly, L. H. *Introduction to Infrared and Raman Spectroscopy*, 3rd ed.; Academic Press: New York, 1990.
(37) Normatov, J.; Silverstein, M. S. *Polymer* **2007**, *48*, 6648.
(38) Gibson, L. J.; Ashby, M. F. *Cellular Solids*, 2nd ed.; Cambridge University Press: Cambridge 1997.
(39) Levental, I.; Georges, P. C.; Janmey, P. A. *Soft Matter* **2007**, *3*, 299.
(40) Saltzman, W. M. *Tissue Engineering: Engineering Principles for the Design of Replacement Organs and Tissues*; Oxford University Press: Oxford, 2004.

MA7027177